

1 TITLE

2

3 EvoWeaver: Large-scale prediction of gene functional associations from coevolutionary
4 signals

5

6 AUTHORS

7

8 Aidan Lakshman¹ and Erik S. Wright^{1,2,*}

9

10 ¹Department of Biomedical Informatics, University of Pittsburgh

11 ²Center for Evolutionary Biology and Medicine, Pittsburgh, PA

12 *address correspondence to eswright@pitt.edu

Preprint, do not distribute

13 ABSTRACT

14

15 The universe of uncharacterized proteins is expanding far faster than our ability to
16 annotate their functions through laboratory study. Computational annotation approaches
17 rely on similarity to previously studied proteins, thereby ignoring unstudied proteins.
18 Coevolutionary approaches hold promise for injecting new information into our
19 knowledge of the protein universe by linking proteins through 'guilt-by-association'.
20 However, existing coevolutionary algorithms have insufficient accuracy and scalability to
21 connect the entire universe of proteins. We present EvoWeaver, an algorithm that
22 weaves together 12 signals of coevolution to quantify the degree of shared evolution
23 between genes. EvoWeaver accurately identifies proteins involved in protein complexes
24 or separate steps of a biochemical pathway. We show the merits of EvoWeaver by
25 partly reconstructing known biochemical pathways without any prior knowledge other
26 than that available from genomic sequences. Applying EvoWeaver to 1,545 gene
27 groups from 8,564 genomes reveals missing connections in popular databases and
28 potentially undiscovered links between proteins.

Preprint, do not distribute

29 INTRODUCTION

30

31 Our ability to capture the protein universe with genome sequencing far outpaces our
32 ability to investigate individual proteins. A select few proteins have historically received
33 a disproportionate amount of study¹⁻³. This annotation inequality hinders biomedical
34 progress by neglecting many proteins that could be important determinants of health⁴.
35 Only a small fraction of uncharacterized proteins can be automatically annotated via
36 similarity to experimentally investigated proteins of known function⁵⁻⁷. The sparsity of
37 high-quality annotations exacerbates the problem of non-specific and low-confidence
38 annotations that proliferate across genomes^{8,9}. Thus, computational approaches to infer
39 function without dependence on prior knowledge are acutely needed.

40 Computationally annotating the remainder of the protein universe requires
41 establishing connections with characterized proteins to generate hypotheses about
42 function through 'guilt by association'¹⁰. Shared function necessitates that protein-
43 encoding genes coevolve in the same cell, thereby leaving behind a molecular signal of
44 coevolution¹¹. Four primary approaches are used to identify coevolution: phylogenetic
45 profiling¹², phylogenetic structure¹³, gene organization¹⁴, and sequence-level methods¹⁵.
46 Each of these coevolutionary signals is an outcome of a shared selection pressure
47 acting on groups of genes. To date, these four coevolutionary approaches have
48 primarily been applied independently. Even large databases of functional associations,
49 such as STRING, only consider evidence from a small subset of coevolutionary
50 approaches¹⁶.

51 Although coevolutionary analyses have shown great potential for predicting functional
52 associations¹⁷⁻²⁴, scalability is a major impediment to comprehensive application on
53 large datasets. The era of big data holds the promise of distinguishing coevolution from
54 other drivers of molecular evolution²⁵. Additionally, holistic evaluation of many
55 coevolutionary signals offers a means of amplifying weaker signals to make higher
56 accuracy predictions. For example, conserved genes will not display a phylogenetic
57 profiling (i.e., presence/absence) signal but may show patterns of gene organization.
58 Combining disparate coevolutionary signals and scaling to larger datasets requires
59 inventing new approaches for discerning signal from noise.

60 Coevolutionary analyses have the potential to infer functional associations directly
61 from sequencing data in a way that is agonistic to prior annotations, thereby overcoming
62 the current reliance on extrapolating from existing knowledge that compounds
63 annotation inequality. Here, we set out to develop a scalable approach to extract and
64 combine coevolutionary signals for predicting functional associations between protein-
65 coding genes. This required improving upon existing approaches to scale to larger input
66 data and incorporate statistical testing. We unite these signals of coevolution using
67 machine learning models to quantify the degree of functional association between
68 genes. Our approach, named EvoWeaver, serves as a high-quality hypothesis
69 generator to help extend our knowledge of the protein universe.

70

71 RESULTS

72

73 Existing coevolutionary algorithms have widespread issues with scalability,
74 interoperability, and interpretability²⁵. We chose to implement all our coevolutionary
75 analyses from scratch within a single software package to standardize user interaction
76 and allow for easy application of ensemble methods. Our approach, named EvoWeaver,
77 takes as input a set of phylogenetic gene trees and optional metadata (Fig. 1a).
78 EvoWeaver then performs four types of coevolutionary analysis, comprised of 12
79 algorithms optimized for scalable performance. These component predictors are
80 combined using a machine learning classifier to compute a strength of coevolution
81 between every pair of gene groups. From this, users can generate novel inferences or
82 hypotheses about gene function.

83 The first type of coevolutionary analysis, phylogenetic profiling, investigates patterns
84 of presence/absence or gain/loss of genes, which manifests when multiple genes work
85 in concert (Fig. 1b). While presence/absence analyses have been successfully used to
86 predict gene function^{12,25-27}, existing approaches are susceptible to biases from small
87 sample sizes or low evolutionary divergence²⁸. We addressed these biases with a novel
88 algorithm (G/L Distance) that examines the distance between gain/loss events to
89 measure compensatory changes rather than extant patterns. We also incorporated
90 statistical testing into existing measures of presence/absence patterns^{12,29} (P/A Info,
91 P/A Jaccard) and correlation of ancestral states³⁰ (G/L Correlation). The end result is a
92 category of algorithms for identifying coevolution between gene groups that are not
93 highly conserved.

94 The second type of coevolutionary analysis, phylogenetic structure, uses the fact that
95 functionally associated genes tend to evolve in tandem, giving rise to similar
96 genealogies (Fig. 1c). Commonly used phylogenetic structure approaches include
97 MirrorTree and ContextTree³¹⁻³³, although these approaches scale poorly due to high
98 computational complexity. We addressed this issue by introducing novel algorithms (RP
99 MirrorTree, RP ContextTree) that use random projection to decrease computational
100 overhead and improve accuracy by reducing redundant information. Random projection
101 provides the added advantage that computation can be distributed across computers,
102 unlike in SVD-phy³⁴, allowing EvoWeaver to process very large datasets on compute
103 clusters. Additionally, we introduce the use of tree distance metrics (Tree Distance) to
104 analyze coevolution via topological differences in genealogies³⁵. Taken together, these
105 algorithms facilitate inference of coevolution among conserved gene groups.

106 The third type of coevolutionary analysis, gene organization, leverages the fact that
107 functionally linked genes tend to colocalize on the genome to facilitate gene regulation
108 and horizontal gene transfer³⁶⁻³⁸ (Fig. 1d). These approaches most commonly employ
109 profile hidden Markov models, such as antiSMASH³⁹⁻⁴¹. While these approaches
110 perform well on functional prediction, they rely on *a priori* knowledge about genes that
111 colocalize. We circumvented this limitation by introducing an algorithm that compares
112 the number of coding regions separating genes (Gene Distance). Our approach is
113 similar to STRING's colocalization metric, which measures the number of nucleotides
114 separating genes¹⁶, but STRING's approach fails to consider that low rates of
115 evolutionary divergence can inflate evidence of colocalization. We address this issue by
116 using Moran's *I* to calculate the extent to which genes remain colocalized in spite of

117 evolutionary divergence. Additionally, EvoWeaver analyzes the conservation of relative
118 transcriptional direction (Transcription Info), since this also indicates functional
119 association⁴². Collectively, these algorithms provide evidence of coevolution among
120 conserved gene groups on the same chromosome.

121 The last type of coevolutionary analysis, sequence-level methods, looks at sequence
122 patterns across gene groups, which are sometimes indicative of physical interactions
123 between gene products⁴³ (Fig. 1e). Direct coupling analysis is a well-known approach in
124 this category⁴⁴⁻⁴⁶, but it suffers from high computational complexity. Instead, we
125 extended a prior approach based on mutual information to predict interacting sites
126 between sequences⁴⁷. EvoWeaver analyzes the extent of these site-wise interactions to
127 construct an overall score (Sequence Info). Additionally, EvoWeaver compares gene
128 sequence natural vectors (Gene Vector), which carry evidence of functional association
129 and can be quickly computed⁴⁸. These algorithms provide additional evidence of
130 coevolution for physically interacting gene products.

131 These four categories span levels of coevolution from the organism (phylogenetic
132 profiling) to the genome (gene organization) to the gene (phylogenetic structure) to the
133 sequence. Since our component analyses individually capture different facets of
134 coevolution, we sought to combine their strengths into a single comprehensive estimate
135 of evidence for functional association between gene pairs. To this end, we trained three
136 machine learning classifiers (logistic regression, random forest, and neural network) on
137 sets of protein-coding gene pairs with known functional associations (Fig. 1a). While
138 these ensemble models require *a priori* knowledge to calibrate their predictions, after
139 training they permit the extension of this knowledge to gene pairs with previously
140 unknown associations and no relationship to the training set.

141

142 **Ensemble methods accurately identify functionally associated genes**

143

144 Selection of high-quality ground truth datasets for coevolutionary analysis is a
145 challenging task²⁵. As with previous studies^{34,49}, we relied upon the Kyoto Encyclopedia
146 of Genes and Genomes database (KEGG) because it is well-curated and
147 experimentally validated^{50,51}. KEGG provides a hierarchical ontology of biochemical
148 pathways consisting of orthologous gene groups (KO groups) participating in protein
149 complexes (Fig. 1f) and/or enzymatic reactions within modules (Fig. 1g). Modules are
150 the building blocks of larger biochemical pathways. We first sought to validate the
151 performance of EvoWeaver at identifying KO groups within the same complex. We
152 anticipated a strong coevolutionary signal for these pairs because of their mutual
153 dependence. Each algorithm's performance was graded on its ability to distinguish 867
154 pairs of KO groups that complex (positives) versus 867 randomly selected pairs of
155 unrelated KO groups (negatives). The negative set was constructed from a weighted
156 random sample of 57,321 unrelated KO groups. Weighted sampling reduces risk of
157 overfitting by matching the distribution of data features in the negative set to the positive
158 set.

159 Almost all coevolution algorithms performed well at identifying KO groups involved in
160 the same complex (Fig. S1). Sequence-level methods performed slightly worse than

161 other categories of coevolutionary signal. This outcome was expected because many
162 non-interacting proteins appear to physically interface similarly to interacting proteins⁵².
163 The predictions of most algorithms were weakly correlated with each other, which
164 suggests combining signals could further improve performance (Fig. S1). To this end,
165 we evaluated three ensemble methods (Logistic Regression, Random Forest, and
166 Neural Network) using five-fold cross validation. All ensemble methods displayed
167 predictive power exceeding component coevolutionary signals, with Random Forest
168 performing the best (Fig. S1).

169 Given EvoWeaver's excellent performance on the Complexes benchmark, we next
170 sought to establish its ability to identify functionally associated protein-coding genes that
171 were not involved in the same protein complex. To this end, we developed the Modules
172 benchmark as a set of 1,948 pairs of gene groups acting in adjacent steps of a
173 biochemical pathway (positives) and 1,948 randomly selected pairs from disconnected
174 pathways (negatives). This task is more challenging because proteins involved in the
175 same module need not physically interact (Fig. 1g). As shown in Figure 2, performance
176 of component algorithms on the Modules benchmark was slightly worse than on the
177 Complexes benchmark. However, ensemble methods retained high performance
178 (AUROC of 0.981 for Random Forest) and greatly outperformed individual
179 coevolutionary signals. The large gap between ensemble and component predictors
180 highlights the importance of using multiple coevolutionary signals to infer functional
181 associations.

182

183 **EvoWeaver infers hierarchical relationships among genes**

184

185 Coevolutionary relationships are stratified across a gradient of associations within the
186 cell. For this reason, it would be ideal to predict a strength of coevolution across a
187 hierarchy of multi-level relationships among gene groups. We evaluated the Random
188 Forest model on pairs of KEGG module blocks belonging to each of five classes: Direct
189 Connection, Same Module, Same Pathway, Same Global Pathway, and Unrelated
190 module blocks. These classes are arranged in a hierarchy of decreasing functional
191 association. Accurate classification would imply EvoWeaver can construct a hierarchical
192 classification scheme of genes and recapitulate the relationships in KEGG. We then
193 used five-fold cross validation to predict class membership for 1,018,353 pairs of
194 module blocks. Most Random Forest predictions were assigned to the correct class or
195 the adjacent class (Fig. S2), even when requiring at least 50% confidence for prediction
196 (Fig. 3a). Unsurprisingly, the model frequently confused the Same Global Pathway and
197 Unrelated classes, which are both expected to contain weakly coevolving genes.

198 EvoWeaver is based on the premise that a comprehensive view of coevolution is
199 preferable to any single source of coevolutionary signal. Along these lines, all 12
200 predictors contributed substantially to the ensemble classifier's accuracy (Fig. 3b). The
201 three top predictors (G/L Correlation, RP ContextTree, and Gene Distance) were also
202 the top predictors in each of the three highest performing categories in the Modules
203 benchmark (Fig. 2). We attributed this observation to the fact that distinct categories of

204 coevolution were generally more weakly correlated with each other (Fig. 2), suggesting
205 they provide complementary information.

206 The Random Forest ensemble classifier was best at distinguishing the top two from
207 bottom three hierarchical classes. Hence, we tested whether these predictions could be
208 used to recapitulate KEGG pathways by building a network of module blocks with
209 connections between pairs predicted as Direct Connection or Same Module. We applied
210 parameter-free label propagation to detect communities within this network⁵³. A
211 randomly selected community is shown in Figure 3c-d, which included all module blocks
212 involved in the prodigiosin biosynthesis pathway. EvoWeaver correctly identified all but
213 two Direct Connections within the pathway and properly distinguished the two modules
214 within the pathway. However, EvoWeaver incorrectly classified some Same Module
215 pairs as Direct Connection, and predicted an element of the actinorhodin biosynthetic
216 pathway (*actIV2,4*) to be involved in this pathway. This was likely a spurious connection
217 due to many *Streptomyces* species producing both actinorhodin and undecylprodigiosin.
218 This result suggests EvoWeaver's predictions can be used to hypothesize biochemical
219 pathways, although EvoWeaver's predictions do not provide directionality to biochemical
220 steps.

221

222 **EvoWeaver outperforms STRING without reliance upon external data**

223

224 STRING is one of the most comprehensive databases of knowledge about
225 functionally associated genes. One of STRING's stated goals⁴⁹ is to predict genes
226 belonging to the same non-global pathway in KEGG, which corresponds to
227 EvoWeaver's Direct Connection, Same Module, and Same Pathway classifications.
228 STRING's Total Score is a composite of seven evidence streams¹⁶. We applied
229 STRING's formula for Total Score to quantify the marginal benefit of each evidence
230 stream. External data, including mining the literature for cooccurrence of terms (Text
231 Mining) and knowledge bases such as KEGG (Databases), provided the majority of
232 STRING's predictive performance (Fig. 4a). EvoWeaver outperformed STRING at its
233 stated goal of predicting pairs of gene groups sharing a functional pathway in KEGG
234 using purely coevolutionary signal without relying on KEGG itself (Fig. 4a). This makes
235 EvoWeaver particularly powerful for identifying unknown functional associations without
236 reliance on prior knowledge, which may help to mitigate the problem of annotation
237 inequality^{1,2}. As expected, STRING's coevolutionary evidence streams (Cooccurrence,
238 Gene Neighborhood) were correlated with comparable signals derived by EvoWeaver
239 (Fig. 4b).

240

241 **EvoWeaver can inform novel hypotheses**

242

243 EvoWeaver's primary purpose is to serve as a generator for novel hypotheses about
244 functional associations. As a proof of concept, we investigated the top 15
245 misclassifications wherein a gene pair was assigned to Direct Connection or Same
246 Module with high confidence when it ostensibly belonged to Same Global Pathway or
247 Unrelated in KEGG (Supplemental Data). While some putative mispredictions had no

248 clear evidence for or against a functional relationship in the literature, several were
249 actually correct predictions between clearly related gene groups that have yet to be
250 connected in the same KEGG module. Several purported mispredictions were for genes
251 encoding proteins involved in closely linked plant biochemical pathways, such as
252 gibberellin and abscisic acid biosynthesis, which are both known to regulate plant
253 dormancy and germination⁵⁴. Other alleged mispredictions were for gene pairs
254 implicated in the same diseases, although there was insufficient experimental evidence
255 to validate their functional association. The existence of quasi-mispredictions implies
256 EvoWeaver can be used to identify errors or voids in our current understanding of
257 molecular biology.

258 As a case study, we examined EvoWeaver's top misprediction, which was between
259 human genes *B3GNT5* and *ST6GAL1*. These genes belong to the "Glycosphingolipid
260 biosynthesis – lacto and neolacto series" and "N-glycan biosynthesis" pathways,
261 respectively. Despite their connection being absent from the KEGG or STRING
262 databases (Fig. 5a), *B3GNT5* was experimentally shown to directly promote the
263 expression of *ST6GAL1* in ovarian cancer cell lines⁵⁵. EvoWeaver predicted this pair to
264 be Direct Connection with probability 0.72 or Same Module with probability 0.27 (Fig.
265 5b). This prediction was supported by weak phylogenetic profiling evidence because of
266 the high conservation of both genes (Fig. 5c), but there was strong evidence for gene
267 organization due to conservation in gene proximity across the phylogeny (Fig. 5d).
268 *B3GNT5* and *ST6GAL1* also displayed strong similarity in their genealogies (Fig. 5e)
269 and moderate evidence for coevolutionary signal at the sequence level (Fig. 5f). This
270 proof of concept demonstrates that EvoWeaver can be used to generate reasonable
271 hypotheses about functional relationships.

272

273 DISCUSSION

274

275 EvoWeaver represents a marked advancement in employing coevolutionary
276 principles to the discovery of functional associations. In this work, we showed that
277 EvoWeaver can capitalize on multiple sources of coevolutionary signal to outcompete
278 individual algorithms at identifying relationships between gene groups. EvoWeaver's
279 accuracy permitted us to construct a multi-level model of functional associations that
280 was able to partly recapitulate experimentally validated KEGG pathways without any
281 prior knowledge of the proteins other than their coding sequences and genomic
282 locations. EvoWeaver's predictive performance was higher than STRING's for the same
283 objective without any dependence on external data. Moreover, we demonstrated how
284 EvoWeaver's predictions can be leveraged to infer novel functional associations that are
285 absent from large databases of biological knowledge.

286 EvoWeaver excels at three characteristics that are necessary for the practical
287 application of coevolutionary analyses on large-scale datasets. First, EvoWeaver is
288 highly scalable owing to its optimized algorithms. We demonstrated this by applying
289 EvoWeaver to 1,545 gene groups from 8,564 genomes across the tree of life. To our
290 knowledge, this is the largest coevolutionary analysis to date, exceeding the 2,167
291 genomes analyzed in previous work^{12,25}. Unlike popular prior approaches, such as

292 ContextTree or SVD-phy^{34,56}, EvoWeaver's pairwise comparisons are independent and
293 can be easily distributed across a cluster of computers. Second, EvoWeaver's
294 predictions are higher accuracy because they incorporate multiple sources of
295 coevolutionary signal, and each component algorithm incorporates statistical testing that
296 mitigates spurious signals. Third, EvoWeaver standardizes the application of multiple
297 algorithms within a single software package with consistent inputs and outputs. This
298 addresses usability issues previously identified in reviews of coevolutionary analyses²⁵.

299 Coevolution differs from protein-protein interactions in that it does not require any
300 physical interaction. There exist many prior approaches to predicting protein-protein
301 interactions, along with databases of known interactors^{45,46,57,58}. Benchmarking
302 functional association algorithms presents its own challenges, as proteins that do not
303 physically interact may nevertheless be functionally associated. This renders common
304 benchmarks for protein-protein interactions insufficient for benchmarking coevolutionary
305 algorithms⁵⁸⁻⁶⁰. We chose to rely on the KEGG database as a source of experimentally
306 validated functional associations within a multi-level hierarchy. Although KEGG is
307 limited in size (i.e., 26,418 orthology groups), it is one of the few comprehensive
308 sources of genomes and genes linked across pathways.

309 We anticipate EvoWeaver to be particularly useful for generating hypotheses that
310 catalyze investigations into understudied proteins. EvoWeaver allows users to search
311 through millions of gene pairs to find a comparatively small number of potential
312 functional associations. EvoWeaver's predictions are particularly valuable when
313 combined with network analyses or expert insights. In the future, EvoWeaver will assist
314 in curating and supplementing large databases of biological knowledge to address
315 errors and annotation inequality. We also expect EvoWeaver's predictions to be useful
316 for other sequence features, such as non-coding RNAs, although protein-coding genes
317 were the focus of this study. Most importantly, EvoWeaver empowers users to combat
318 annotation inequality by predicting functional associations for the rapidly expanding
319 collection of sequences with unknown function.

320 ONLINE METHODS

321

322 **Construction of Benchmark Datasets**

323

324 The goal of the Complexes benchmark is to judge algorithms' ability to discern genes
325 encoding proteins involved a complex versus genes encoding unrelated proteins. To
326 this end, we identified all orthology groups belonging to a complex in KEGG⁶¹, for a total
327 of 372 gene groups. We computed pairwise coevolutionary scores between orthology
328 groups with at least three sequences that were involved in a complex, for a total of 358
329 orthology groups. This resulted in 57,321 pairs that are not in the same pathway
330 (unrelated pairs) and 867 pairs participating as required or optional components of the
331 same complex. Positive pairs were defined as the 867 pairs from the same complex,
332 and an equivalent number of negative pairs were drawn to create a balanced dataset for
333 benchmarking. Random sampling of negative pairs was weighted in order to match the
334 distribution in number of sequences per gene group to that of the positive pairs. This
335 weighted sampling was used to mitigate the ability of algorithms to use the number of
336 sequences per group as a proxy for functional association.

337 Next, we constructed the Modules benchmark to test algorithms' ability to discern
338 proteins acting in subsequent steps of a biochemical pathway versus unrelated proteins.
339 We first identified all module blocks within the KEGG MODULES database. Each
340 module block is a set of one or more orthology groups that perform a discrete step
341 within a biochemical pathway (Fig. 1g). Each module was parsed from its definition on
342 KEGG (Table S1), for a total of 369 modules. Positive test cases were defined as
343 successive blocks in a module, and negative cases were defined as module blocks in
344 separate modules not sharing a pathway in KEGG. Global and Overview Pathways
345 were not considered, since their broad definition encompasses most proteins in KEGG.
346 Blocks containing complexes were also excluded to prevent overlap with the Complexes
347 benchmark. Since some orthology groups belong to multiple blocks, only pairs of blocks
348 without overlap in orthology groups were assessed. The final Modules benchmark was
349 comprised of 1,545 blocks with 1,948 positive pairs. An equivalent number of negative
350 pairs were sampled in the same manner as the Complexes benchmark.

351 Having constructed two binary benchmarks, we sought to explore EvoWeaver's
352 ability to distinguish interaction strengths among proteins. Accordingly, we used the
353 relationships encoded in the KEGG PATHWAYS database to define multiple
354 hierarchical levels of functional association. We assigned all pairs of module blocks into
355 one of five categories: Direct Connection, Same Module, Same Pathway, Same Global
356 Pathway, or Unrelated. The Same Pathway group comprises pairs of module blocks
357 that share a pathway not in the Global and Overview Pathways category in KEGG, and
358 the Unrelated group comprises pairs with no modules or pathways in common. We
359 chose 50% confidence as the cutoff for classification (Fig. 3a) because these
360 predictions have higher probability assigned to their predicted category than their sum
361 of probabilities across all other categories. The confusion matrix at 0% confidence is
362 shown in Figure S2. To look for novel connections (Fig. 5), we examined pairs

363 belonging to Unrelated and Same Global Pathway groups that EvoWeaver predicted as
364 being Direct Connection or Same Module.

365

366 **Preparing Gene Groups for Analysis**

367

368 EvoWeaver takes as input a set of two or more gene trees, which may include
369 sequences, gene indexes, and/or a species tree. It then applies the set of component
370 algorithms for which it has the necessary input data types. We obtained amino acid
371 sequences for each gene group from KEGG and used DECIPHER⁶² to trim paralogs,
372 align sequences, and construct neighbor joining gene trees. In total, there were 8,564
373 genomes with at least one gene present in the benchmarks. Species trees were
374 estimated using the ASTRID algorithm⁶³. To find each gene's index within its genome,
375 we downloaded complete genomes and coding sequences from NCBI following the
376 reference links provided in KEGG. Of the 8,564 genomes present in the benchmarks,
377 7,535 had genome sequences available. Coding sequences were matched to locations
378 on the genome with the *Biostrings* (v2.68.1) package in R^{64,65} (v4.3.0).

379

380 **Coevolutionary Algorithms in EvoWeaver**

381

382 The goal of EvoWeaver is to capture a holistic view of coevolution for predicting
383 functional associations between groups of genes. To achieve this, we implemented 12
384 algorithms from scratch that quantify different sources of coevolutionary signal. Each
385 algorithm analyzes a pair of gene groups and returns a score between zero and one,
386 where zero represents an absence of signal and more positive values imply greater
387 coevolutionary signal. Some algorithms can provide scores between -1 and 1, in which
388 case rare negative scores represent an inverse coevolutionary association. To correct
389 for spurious signal resulting from insufficient information, we multiply all scores by their
390 significance ($1 - p\text{-value}$). The resulting scores are combined into an overall prediction
391 using an ensemble machine learning method. When an algorithm cannot make a
392 prediction for a particular pair, the score passed to the ensemble method for that
393 algorithm is zero. For example, if a pair of genes do not cooccur in any organisms, then
394 their score for all gene organization algorithms is zero. The 12 algorithms implemented
395 fall into four categories: phylogenetic profiling, phylogenetic structure, gene
396 organization, and sequence-level methods (Fig. 1a). Of these, four algorithms are
397 completely novel (G/L Distance, RP ContextTree, RP MirrorTree, and Gene Distance),
398 three are novel applications of existing algorithms (TreeDistance, Moran's I, Gene
399 Vector), and the remaining five are refinements on existing algorithms.

400

401 *Phylogenetic Profiling*

402

403 Phylogenetic profiling is a common technique that uses presence/absence (P/A)
404 profiles of genes to investigate shared function. The approaches previously introduced
405 in the literature use binary P/A profiles, where one represents the presence of a gene
406 and zero represents its absence⁶⁶. The first P/A approach used Hamming distances on
406 binary profiles as a score⁶⁷. Later, Jaccard index and mutual information were applied to

407 score P/A profiles^{12,68}. Subsequent work transformed P/A profiles into ancestral
408 gain/loss (G/L) events and scored the correlation between events³⁰. This transformation
409 reduces redundancy for sets of organisms with low rates of gene gain and loss^{28,30}.

410 EvoWeaver includes four phylogenetic profiling algorithms (Fig. 1b). The first
411 algorithm, P/A MI, calculates bidirectional mutual information of binary P/A profiles using
412 a recently introduced weighting scheme⁶⁹. The second algorithm, P/A Jaccard, uses the
413 Jaccard index of P/A profiles. The third algorithm, G/L Correlation, applies Fitch
414 Parsimony⁷⁰ to infer ancestral states on the species tree from P/A profiles. These G/L
415 profiles include three states: -1 for gene loss, 0 for no change, and +1 for gene gain.
416 The G/L Correlation score is defined as Pearson's correlation coefficient of the ternary
417 G/L profiles.

418 G/L Correlation fails to account for compensatory changes that do not occur on the
419 same branch of the species tree, which are common in sequence evolution⁷¹. The fourth
420 algorithm, G/L Distance, quantifies the evolutionary distance between G/L events
421 assuming the time between gain or loss events is exponentially distributed. Thus, the
422 score between a pair of events for two gene groups is calculated as $w e^{-d(v_1, v_2)}$, where w
423 is +1 if the events are the same (i.e., both gain or both loss) and -1 if the events are
424 different, and $d(v_1, v_2)$ is the distance between events v_1 and v_2 on the species tree.
425 The distance between events on separate branches is defined as the total distance
426 between their branch midpoints. The distance between events on the same branch is
427 defined as the expected value of distance between two points randomly placed on a line
428 segment (i.e., $1/3^{\text{rd}}$ the branch length). For each pair of genes, events are paired to their
429 closest event from the other group. The total score for the gene pair is the average
430 score for all event pairs, and ranges from -1 to +1.

431 Statistical significance for P/A MI, P/A Jaccard, and G/L Correlation are calculated
432 using Fisher's Exact Test (two-way for P/A and three-way for G/L), and a p-value for
433 G/L Distance is calculated using empirical values from permutation testing with 100
434 replicates.

435

436 *Phylogenetic Structure*

437 Gene tree structural comparisons were pioneered by MirrorTree³², which scores each
438 pair of gene groups by the correlation of their pairwise sequence distances. Subsequent
439 improvements to MirrorTree attempted to correct for background evolutionary signal
440 prior to analysis⁷². These extensions, often referred to as ContextTree or ContextMirror,
441 use different approaches to remove shared signal represented by the species
442 tree^{31,56,73}. More recently, SVD-phy was introduced as an alternative approach using
443 BLAST to measure distance between sequences^{34,74}. SVD-phy uses singular value
444 decomposition to reduce redundant information contained in pairwise distances, which
445 removes signal shared across all genes and improves overall predictions. However, this
446 approach requires that all pairwise distances be simultaneously kept in memory.

447 EvoWeaver uses random projection in lieu of SVD for dimensionality reduction.
448 Random projection is a surjective mapping that approximately preserves distances
449 between vectors⁷⁵. While traditional random projection uses a large matrix of random
450 values, this requirement can be circumvented by generating values of the matrix on the

451 fly with a preset random seed. Hence, this dimensionality reduction can be done with
452 negligible memory overhead, allowing for efficient and replicable distribution across a
453 compute cluster. The RP MirrorTree algorithm applies random projection to patristic
454 distances and scores pairs of vectors using Spearman's correlation coefficient. The RP
455 ContextTree algorithm also subtracts the randomly projected species tree from each
456 vector prior to scoring. RP ContextTree's final scores are multiplied by the Jaccard
457 index of overlap in organism membership to correct for spurious correlations caused by
458 minimally overlapping sets. Statistical significance for both RP ContextTree and RP
459 MirrorTree are calculated using the closed form solution for significance of Spearman's
460 correlation coefficient.

461 EvoWeaver also incorporates tree distance metrics to measure topological similarity.
462 A variety of previously benchmarked metrics³⁵ were implemented as measures of
463 functional similarity, all of which were highly correlated in their tree distances. By
464 default, EvoWeaver's TreeDistance predictor uses normalized Robinson-Foulds
465 Distance due to its low memory requirement and closed form solution for significance⁷⁶.
466 The score for each pair of genes was defined as $1 - TD(T_1, T_2)$, where TD is the tree
467 distance and T_1 and T_2 are gene trees.

468 *Gene Organization*

469 Gene organization is commonly used as a signature of functional association. For
470 example, *a priori* knowledge of genes that colocalize can be used to find biosynthetic
471 gene clusters. Existing programs, such as antiSMASH³⁹, use profile hidden Markov
472 models to search for clusters of genes with known functional associations. However,
473 these approaches cannot be used to find gene clusters *de novo*. STRING makes use of
474 the distance in nucleotides between genes as a *de novo* predictor of functional
475 association¹⁶. To our knowledge, analysis of gene organization is one of the most
476 understudied approaches for *de novo* prediction of functional associations.

477 EvoWeaver incorporates three gene organization algorithms. Together, they provide
478 a well-rounded view of gene organization: the first algorithm looks at whether genes are
479 possibly transcribed together, the second measures how closely genes are located to
480 each other, and the third quantifies the extent to which gene distances are preserved
481 across phylogenies. The first algorithm, Transcription MI, examines the relative
482 transcriptional direction of gene pairs. Conservation of transcriptional direction has been
483 validated in prior work to be indicative of shared function⁷⁷. The score for Transcription
484 MI is defined as the bidirectional mutual information⁶⁹ between transcriptional directions
485 of gene pairs, with Fisher's Exact Test used to determine statistical significance.

486 The second algorithm, Gene Distance, examines the separation between genes. For
487 each pair of genes on the same chromosome, the distance d is calculated as the
488 absolute value of the difference in gene index. The index of a gene is its gene order in
489 the chromosome, starting from one for the first gene. We used indices rather than
490 nucleotide locations to mitigate the effect of variability in gene lengths. The score for
491 each pair of sequences is defined as e^{1-d} , and the overall score for a pair of gene
492 groups is the mean of their sequence pair scores. In this way, Gene Distance is
493 maximized (1) when two genes are always adjacent ($d = 1$). Statistical significance is
494

495 derived from the distribution of distances between two random points on a line
496 segment⁷⁸.

497 The third algorithm, Moran's I , measures spatial autocorrelation among gene
498 distances. Moran's I requires pairwise weights represented by the inverse exponential
499 of the patristic distances⁷⁹ and values in the form of gene distances (d). Moran's I
500 distinguishes between genes that are colocated purely due to low evolutionary
501 divergence versus genes that have maintained a consistent relative distance in spite of
502 evolutionary divergence. Statistical significance is calculated using the closed form
503 solution to the expected value and variance of Moran's I (ref. ⁸⁰).

504

505 *Sequence-Level Methods*

506 Covariation of residues is a common signal of protein-protein interactions, and
507 numerous methods have been devised for this purpose. A popular approach is direct
508 coupling analysis⁴⁶, which fits a Potts model to a multiple sequence alignment in order
509 to parse "direct effects" from "indirect effects." Other algorithms using deep learning
510 have been successfully applied to sequencing data for finding interaction sites between
511 proteins^{81,82}. While some previously developed approaches improved scaling^{83,84}, many
512 of these algorithms have prohibitively high computational complexity for high-throughput
513 analysis. Additionally, the focus of these algorithms is on finding interaction sites
514 between small numbers of proteins or proteins known *a priori* to have a high likelihood
515 of interacting.

516 EvoWeaver implements two sequence-level methods. The first of these, Gene
517 Vector, uses the gene sequence natural vector approach, developed to predict protein-
518 protein interactions⁴⁸. We extended this algorithm to amino acids following the same
519 theoretical model as the initial nucleotide-based method. We chose to use the natural
520 vector without 2-mers or 3-mers, since the full vector incurred high computational
521 overhead with a negligible difference in scores. For each pair of gene groups, we subset
522 the sequences to the intersection of the organisms present in both groups. The natural
523 vector for each group in the pair is the average of the natural vectors for each of its
524 constituent sequences. We centered each natural vector assuming a null model of
525 equally distributed nucleotides or amino acids. The final score and statistical
526 significance for the pairing are calculated from Spearman's correlation coefficient of the
527 natural vectors.

528 The second approach, Sequence Info, extends a prior approach to measure the
529 mutual information between sites within sequence alignments of each gene group⁴⁷. For
530 every pair of gene groups, we subset the sequences to the genomes that appear in both
531 groups, and subset the sites to those with high information content (entropy ≥ 0.3 bits)
532 using the *MaskAlignment* function in DECIPHER⁶². Mutual information is calculated for
533 each pair of sites (i.e., columns) across both alignments after applying a background
534 entropy correction along with an average product correction⁸⁵. The final score is
535 calculated as the average of the highest scoring pairing for each site. Statistical
536 significance is calculated by applying Fisher's combined probability test to the
537 distribution of p-values across sites.

538

539 *Ensemble Methods*

540 EvoWeaver combines the output of each of the aforementioned coevolutionary
541 algorithms into a final prediction using an ensemble machine learning method. All 12
542 algorithms were used as features for ensemble prediction (Fig. 2). For ensemble
543 methods, we tested logistic regression, random forest, and neural network models in
544 R⁶⁵. Logistic regression was performed with the *glm* function, random forests using
545 default parameters in the *randomForest* package⁸⁶ (v4.7-1.1), and neural networks
546 using the *neuralnet* package (v1.44.2). The neural network architecture was a feed
547 forward network with 12 inputs, one hidden layer of matched size (i.e., 12), two output
548 nodes (i.e., class=0 or class=1), and sigmoid activation functions on each node. We
549 intentionally chose relatively simple architectures with default parameters for our
550 ensemble models to maintain interpretability of the predictions and mitigate overfitting to
551 the dataset. All models were evaluated using 5-fold cross validation without
552 hyperparameter tuning.

553 Only random forest was used for hierarchical classification due to its better
554 performance in the binary classification benchmarks. Hierarchical classification was also
555 evaluated using 5-fold cross validation. Members of each class were distributed equally
556 among each train/test fold. To prevent overfitting from high class imbalance in the
557 complete dataset, we downsampled classes in each training set to match the size of the
558 smallest class, Direct Connection, with 1,948 members. This meant that each class in
559 the train set for each fold had 1,558 members (i.e., 80%). Testing was done on the
560 complete (unbalanced) test set, which comprised 203,669 - 203,674 members (i.e.,
561 ~20%) per fold. Each pair was in exactly one test set. Feature importance for the
562 random forest model was calculated using permutation importance, which was chosen
563 over mean decrease in Gini impurity since the latter has been shown to produce biased
564 estimates⁸⁷.

565 To construct an example network, we first created a weighted adjacency matrix from
566 the random forest predictions. Each node represented a single gene group and was
567 connected to its top two Direct Connection predictions with edges of weight 1.0. All
568 predicted Same Module pairs were connected with edges of weight 0.5. Our basis for
569 this approach is that most nodes in KEGG are directly connected to two neighbors, and
570 other nodes in the same module are less important than direct connections. We then
571 used label propagation implemented in the *igraph* package⁸⁸ (v1.5.0.1) to perform
572 community detection. The network in Fig. 3c was randomly chosen from the resulting
573 communities.

574 A possible concern with holding out pairs in cross validation is that ensemble
575 methods could use spurious signals to simply distinguish highly connected gene groups
576 from less connected groups. We further validated our results by reevaluating our
577 ensemble classifier using 10-fold cross validation with gene group holdouts rather than
578 pair holdouts. Within each fold, 10% of gene groups were randomly selected, and all
579 pairs involving at least one of these groups was taken as the test set. The resulting
580 train/test sets each comprised roughly 80/20% of the data (respectively), which forms a
581 comparable scenario to 5-fold cross validation with pair holdouts. The results of this
582 classification were virtually identical to prior results (Fig. S3), implying that EvoWeaver

583 is not heavily relying on features of the individual gene groups themselves when making
584 predictions. This is consistent with the notion that most gene groups have few direct
585 connections and thus learning to distinguish highly connected gene groups gives little
586 predictive power.

587

588 **Comparison with STRING**

589

590 Data for STRING's clusters of orthologous genes (COGs) and interactions were
591 downloaded from STRING v12.0. Since STRING's COG membership sometimes did not
592 perfectly correspond to KEGG's KO groups, we tabulated the KO group assignments for
593 sequences belonging to each STRING COG. Overall, 6,849 COGs had at least one
594 sequence that could be mapped to a KO group in KEGG. Each STRING COG was
595 mapped to KEGG Module blocks using its majority ($\geq 50\%$) KEGG KO group. A total of
596 6,311 COGs had a majority KO group, and 4,481 (71%) of these COGs had perfect
597 consensus. Only 538 STRING COGs lacked a consensus KO group, and these COGs
598 were excluded from analysis.

599 STRING's stated goal for its Total Score is to estimate how likely a reported
600 functional linkage between two proteins "is at least as specific as that between an
601 average pair of proteins annotated on the same 'map' or 'pathway' in KEGG"⁴⁹.
602 Therefore, EvoWeaver's analogous predictions were made by summing the probabilities
603 predicted for Direct Connection, Same Module, and Same Pathway in the hierarchical
604 classification (Fig. 3). A total of 3,446 pairs of COGs in the matched dataset belonged to
605 the Same Pathway, Same Module, or Direct Connection categories in KEGG. An
606 equivalent number of negatives were randomly sampled from the remaining pairs in a
607 similar manner to the Modules benchmark. STRING provides its Total Score calculation
608 within a Python script available on their website. We used this formula to calculate the
609 hypothetical Total Score using subsets of STRING's evidence streams. The sequence
610 of AUROCs in Figure 4a was obtained by sequentially adding the evidence stream with
611 the lowest impact on AUROC to the Total Score calculation.

612

613 **Experimental Details**

614

615 All analysis and plotting was performed with R (v4.3.0). Area under receiver operator
616 characteristic curves and precision-recall curves were calculated with the *auc* function in
617 the *DescTools* package (v0.99.49) for R. Algorithms were implemented in EvoWeaver
618 using R and C programming languages, with user-exposed methods available in R via
619 the *SynExtend* package (v1.16.0). SynExtend is dependent on the *DECIPHER* package
620 (v2.28.0) and is distributed via the Bioconductor software repository⁸⁹. Users can run
621 EvoWeaver by initializing an EvoWeaver object in R with the *EvoWeaver* function, and
622 then using the *predict* function to run component algorithms. Local analyses were
623 performed on a MacBook Pro with M1 Pro CPU and 32GB of RAM. Distributed
624 computing was performed on the Open Science Grid⁹⁰. Phylogenetic tree reconstruction
625 used eight core nodes with 8 - 16GB RAM and 8GB disk space, and pairwise
626 coevolutionary score calculations with EvoWeaver used single core nodes with 2 - 4GB

627 RAM and 2 - 4GB disk space. Computers matching these node specifications varied
628 based on availability and Open Science Grid scheduling. Scripts for reproducing all
629 analyses are available on GitHub (<https://github.com/WrightLabScience/EvoWeaver-ExampleCode>). Datasets are available from Zenodo (DOI: 10.5281/zenodo.10266140).

631

632 ACKNOWLEDGEMENTS

633

634 This study was funded by the NIAID at the NIH (grant number 1U01AI176418-01). AHL
635 was supported by the NLM at the NIH (award number 5T15LM007059-35). This
636 research was done using services provided by the OSG Consortium. Figures 1, 3, and 5
637 were created using BioRender.

638

639 REFERENCES

640

- 641 1 Kustatscher, G. *et al.* Understudied proteins: opportunities and challenges for
642 functional proteomics. *Nature Methods* (2022). [https://doi.org:10.1038/s41592-](https://doi.org:10.1038/s41592-022-01454-x)
643 [022-01454-x](https://doi.org:10.1038/s41592-022-01454-x)
- 644 2 Kustatscher, G. *et al.* An open invitation to the Understudied Proteins Initiative.
645 *Nature Biotechnology* (2022). <https://doi.org:10.1038/s41587-022-01316-z>
- 646 3 Sinha, S., Eisenhaber, B., Jensen, L. J., Kalbuajji, B. & Eisenhaber, F. Darkness
647 in the Human Gene and Protein Function Space: Widely Modest or Absent
648 Illumination by the Life Science Literature and the Trend for Fewer Protein
649 Function Discoveries Since 2000. *PROTEOMICS* **18**, 1800093 (2018).
650 <https://doi.org:10.1002/pmic.201800093>
- 651 4 Haynes, W. A., Tomczak, A. & Khatri, P. Gene annotation bias impedes
652 biomedical research. *Scientific Reports* **8** (2018). [https://doi.org:10.1038/s41598-](https://doi.org:10.1038/s41598-018-19333-x)
653 [018-19333-x](https://doi.org:10.1038/s41598-018-19333-x)
- 654 5 Salzberg, S. L. Next-generation genome annotation: we still struggle to get it
655 right. *Genome Biology* **20** (2019). <https://doi.org:10.1186/s13059-019-1715-2>
- 656 6 Lobb, B., Tremblay, B. J.-M., Moreno-Hagelsieb, G. & Doxey, A. C. An
657 assessment of genome annotation coverage across the bacterial tree of life.
658 *Microbial Genomics* **6** (2020). <https://doi.org:10.1099/mgen.0.000341>
- 659 7 Stoeger, T., Gerlach, M., Morimoto, R. I. & Nunes Amaral, L. A. Large-scale
660 investigation of the reasons why potentially important genes are ignored. *PLOS*
661 *Biology* **16**, e2006643 (2018). <https://doi.org:10.1371/journal.pbio.2006643>
- 662 8 Schnoes, A. M., Ream, D. C., Thorman, A. W., Babbitt, P. C. & Friedberg, I.
663 Biases in the Experimental Annotations of Protein Function and Their Effect on
664 Our Understanding of Protein Function Space. *PLoS Computational Biology* **9**,
665 e1003063 (2013). <https://doi.org:10.1371/journal.pcbi.1003063>
- 666 9 Gillis, J. & Pavlidis, P. The Impact of Multifunctional Genes on "Guilt by
667 Association" Analysis. *PLoS ONE* **6**, e17258 (2011).
668 <https://doi.org:10.1371/journal.pone.0017258>
- 669 10 Aravind, L. Guilt by association: contextual information in genome analysis.
670 *Genome Research* **10**, 1074-1077 (2000).

- 671 11 Codoñer, F. M. & Fares, M. A. Why should we care about molecular coevolution?
672 *Evol Bioinform Online* **4**, 29-38 (2008).
- 673 12 Moi, D., Kilchoer, L., Aguilar, P. S. & Dessimoz, C. Scalable phylogenetic
674 profiling using MinHash uncovers likely eukaryotic sexual reproduction genes.
675 *PLOS Computational Biology* **16**, e1007553 (2020).
676 <https://doi.org:10.1371/journal.pcbi.1007553>
- 677 13 Kann, M. G., Shoemaker, B. A., Panchenko, A. R. & Przytycka, T. M. Correlated
678 Evolution of Interacting Proteins: Looking Behind the Mirrortree. *Journal of*
679 *Molecular Biology* **385**, 91-98 (2009). <https://doi.org:10.1016/j.jmb.2008.09.078>
- 680 14 Umemura, M., Koike, H. & Machida, M. Motif-independent de novo detection of
681 secondary metabolite gene clusters-toward identification from filamentous fungi.
682 *Front Microbiol* **6**, 371-371 (2015). <https://doi.org:10.3389/fmicb.2015.00371>
- 683 15 Feinauer, C., Szurmant, H., Weigt, M. & Pagnani, A. Inter-Protein Sequence Co-
684 Evolution Predicts Known Physical Interactions in Bacterial Ribosomes and the
685 Trp Operon. *PLOS ONE* **11**, e0149166 (2016).
686 <https://doi.org:10.1371/journal.pone.0149166>
- 687 16 Szklarczyk, D. *et al.* The STRING database in 2021: customizable protein-
688 protein networks, and functional characterization of user-uploaded
689 gene/measurement sets. *Nucleic Acids Research* **49**, D605-D612 (2021).
690 <https://doi.org:10.1093/nar/gkaa1074>
- 691 17 Stupp, D., Sharon, E., Bloch, I., Zitnik, M., Zuk, O. & Tabach, Y. Co-evolution
692 based machine-learning for predicting functional interactions between human
693 genes. *Nature Communications* **12** (2021). [https://doi.org:10.1038/s41467-021-](https://doi.org:10.1038/s41467-021-26792-w)
694 [26792-w](https://doi.org:10.1038/s41467-021-26792-w)
- 695 18 Tabach, Y. *et al.* Human disease locus discovery and mapping to molecular
696 pathways through phylogenetic profiling. *Molecular systems biology* **9**, 692
697 (2013).
- 698 19 Tabach, Y. *et al.* Identification of small RNA pathway genes using patterns of
699 phylogenetic conservation and divergence. *Nature* **493**, 694-698 (2013).
- 700 20 Sherill-Rofe, D. *et al.* Mapping global and local coevolution across 600 species to
701 identify novel homologous recombination repair genes. *Genome Research* **29**,
702 439-448 (2019). <https://doi.org:10.1101/gr.241414.118>
- 703 21 Andreo-Vidal, A., Binda, E., Fedorenko, V., Marinelli, F. & Yushchuk, O. Genomic
704 Insights into the Distribution and Phylogeny of Glycopeptide Resistance
705 Determinants within the Actinobacteria Phylum. *Antibiotics (Basel)* **10** (2021).
706 <https://doi.org:10.3390/antibiotics10121533>
- 707 22 Ding, D. *et al.* Co-evolution of interacting proteins through non-contacting and
708 non-specific mutations. *Nature Ecology & Evolution* (2022).
709 <https://doi.org:10.1038/s41559-022-01688-0>
- 710 23 Fongang, B., Zhu, Y., Wagner, E. J., Kudlicki, A. & Rowicka, M. *Co-evolutionary*
711 *analysis accurately predicts details of interactions between the Integrator*
712 *complex subunits* (Cold Spring Harbor Laboratory, 2019).

- 713 24 Ramani, A. K. & Marcotte, E. M. Exploiting the Co-evolution of Interacting
714 Proteins to Discover Interaction Specificity. *Journal of Molecular Biology* **327**,
715 273-284 (2003). [https://doi.org/10.1016/S0022-2836\(03\)00114-1](https://doi.org/10.1016/S0022-2836(03)00114-1)
- 716 25 Moi, D. & Dessimoz, C. Phylogenetic profiling in eukaryotes comes of age.
717 *Proceedings of the National Academy of Sciences* **120** (2023).
718 <https://doi.org/10.1073/pnas.2305013120>
- 719 26 Fukunaga, T. & Iwasaki, W. Inverse Potts model improves accuracy of
720 phylogenetic profiling. *Bioinformatics* **38**, 1794-1800 (2022).
721 <https://doi.org/10.1093/bioinformatics/btac034>
- 722 27 Cheng, Y. & Perocchi, F. ProtPhylo: identification of protein–phenotype and
723 protein–protein functional associations via phylogenetic profiling. *Nucleic Acids*
724 *Research* **43**, W160-W168 (2015). <https://doi.org/10.1093/nar/gkv455>
- 725 28 Škunca, N. & Dessimoz, C. Phylogenetic profiling: how much input data is
726 enough? *PloS one* **10**, e0114701 (2015).
- 727 29 Mering, C. V. STRING: a database of predicted functional associations between
728 proteins. *Nucleic Acids Research* **31**, 258-261 (2003).
729 <https://doi.org/10.1093/nar/gkg034>
- 730 30 Dembech, E. *et al.* Identification of hidden associations among eukaryotic genes
731 through statistical analysis of coevolutionary transitions. *Proceedings of the*
732 *National Academy of Sciences* **120** (2023).
733 <https://doi.org/10.1073/pnas.2218329120>
- 734 31 Pazos, F., Ranea, J. A., Juan, D. & Sternberg, M. J. Assessing protein co-
735 evolution in the context of the tree of life assists in the prediction of the
736 interactome. *J Mol Biol* **352**, 1002-1015 (2005).
737 <https://doi.org/10.1016/j.jmb.2005.07.005>
- 738 32 Pazos, F. & Valencia, A. Similarity of phylogenetic trees as indicator of protein–
739 protein interaction. *Protein Engineering, Design and Selection* **14**, 609-614
740 (2001). <https://doi.org/10.1093/protein/14.9.609>
- 741 33 Clark, G. W., Dar, V.-U.-N., Bezginov, A., Yang, J. M., Charlebois, R. L. & Tillier,
742 E. R. M. 237-256 (Humana Press, 2011).
- 743 34 Franceschini, A., Lin, J., von Mering, C. & Jensen, L. J. SVD-phy: improved
744 prediction of protein functional associations through singular value decomposition
745 of phylogenetic profiles. *Bioinformatics* **32**, 1085-1087 (2016).
- 746 35 Smith, M. R. Information theoretic generalized Robinson–Foulds metrics for
747 comparing phylogenetic trees. *Bioinformatics* **36**, 5007-5013 (2020).
748 <https://doi.org/10.1093/bioinformatics/btaa614>
- 749 36 Rokas, A., Wisecaver, J. H. & Lind, A. L. The birth, evolution and death of
750 metabolic gene clusters in fungi. *Nature Reviews Microbiology* **16**, 731-744
751 (2018). <https://doi.org/10.1038/s41579-018-0075-3>
- 752 37 Perival, V. & Scaria, V. Insights into structural variations and genome
753 rearrangements in prokaryotic genomes. *Bioinformatics* **31**, 1-9 (2014).
754 <https://doi.org/10.1093/bioinformatics/btu600>
- 755 38 Rocha, E. P. The organization of the bacterial genome. *Annual review of*
756 *genetics* **42**, 211-233 (2008).

- 757 39 Blin, K. *et al.* antiSMASH 6.0: improving cluster detection and comparison
758 capabilities. *Nucleic Acids Research* **49**, W29-W35 (2021).
759 <https://doi.org:10.1093/nar/gkab335>
- 760 40 Kautsar, S. A., Suarez Duran, H. G., Blin, K., Osbourn, A. & Medema, M. H.
761 plantiSMASH: automated identification, annotation and expression analysis of
762 plant biosynthetic gene clusters. *Nucleic acids research* **45**, W55-W63 (2017).
763 <https://doi.org:10.1093/nar/gkx305>
- 764 41 Kautsar, S. A., Blin, K., Shaw, S., Weber, T. & Medema, M. H. BiG-FAM: the
765 biosynthetic gene cluster families database. *Nucleic Acids Res* **49**, D490-d497
766 (2021). <https://doi.org:10.1093/nar/gkaa812>
- 767 42 Davila Lopez, M., Martinez Guerra, J. J. & Samuelsson, T. Analysis of gene
768 order conservation in eukaryotes identifies transcriptionally and functionally
769 linked genes. *PloS one* **5**, e10654 (2010).
- 770 43 Thomas, J., Ramakrishnan, N. & Bailey-Kellogg, C. Graphical models of protein-
771 protein interaction specificity from correlated mutations and interaction data.
772 *Proteins: Structure, Function, and Bioinformatics* **76**, 911-929 (2009).
773 <https://doi.org:10.1002/prot.22398>
- 774 44 Morcos, F., Hwa, T., Onuchic, J. N. & Weigt, M. Direct coupling analysis for
775 protein contact prediction. *Methods Mol Biol* **1137**, 55-70 (2014).
776 https://doi.org:10.1007/978-1-4939-0366-5_5
- 777 45 Morcos, F. *et al.* Direct-coupling analysis of residue coevolution captures native
778 contacts across many protein families. *Proceedings of the National Academy of*
779 *Sciences* **108**, E1293-E1301 (2011).
- 780 46 Weigt, M., White, R. A., Szurmant, H., Hoch, J. A. & Hwa, T. Identification of
781 direct residue contacts in protein-protein interaction by message passing.
782 *Proceedings of the National Academy of Sciences* **106**, 67-72 (2009).
783 <https://doi.org:10.1073/pnas.0805923106>
- 784 47 Martin, L. C., Gloor, G. B., Dunn, S. D. & Wahl, L. M. Using information theory to
785 search for co-evolving residues in proteins. *Bioinformatics* **21**, 4116-4124 (2005).
786 <https://doi.org:10.1093/bioinformatics/bti671>
- 787 48 Zhao, N., Zhuo, M., Tian, K. & Gong, X. Protein-protein interaction and non-
788 interaction predictions using gene sequence natural vector. *Communications*
789 *Biology* **5** (2022). <https://doi.org:10.1038/s42003-022-03617-0>
- 790 49 Szklarczyk, D. *et al.* The STRING database in 2011: functional interaction
791 networks of proteins, globally integrated and scored. *Nucleic Acids Research* **39**,
792 D561-D568 (2011). <https://doi.org:10.1093/nar/gkq973>
- 793 50 Kanehisa, M. KEGG: Kyoto Encyclopedia of Genes and Genomes. *Nucleic Acids*
794 *Research* **28**, 27-30 (2000). <https://doi.org:10.1093/nar/28.1.27>
- 795 51 Kanehisa, M., Sato, Y., Furumichi, M., Morishima, K. & Tanabe, M. New
796 approach for understanding genome variations in KEGG. *Nucleic Acids Res* **47**,
797 D590-d595 (2019). <https://doi.org:10.1093/nar/gky962>
- 798 52 Launay, G., Ceres, N. & Martin, J. Non-interacting proteins may resemble
799 interacting proteins: prevalence and implications. *Scientific Reports* **7**, 40419
800 (2017). <https://doi.org:10.1038/srep40419>

801 53 Raghavan, U. N., Albert, R. & Kumara, S. Near linear time algorithm to detect
802 community structures in large-scale networks. *Phys Rev E Stat Nonlin Soft*
803 *Matter Phys* **76**, 036106 (2007). <https://doi.org:10.1103/PhysRevE.76.036106>
804 54 Tuan, P. A., Kumar, R., Rehal, P. K., Toora, P. K. & Ayele, B. T. Molecular
805 mechanisms underlying abscisic acid/gibberellin balance in the control of seed
806 dormancy and germination in cereals. *Frontiers in Plant Science* **9**, 668 (2018).
807 55 Alam, S. *et al.* Altered (neo-) lacto series glycolipid biosynthesis impairs α -6
808 sialylation on N-glycoproteins in ovarian cancer cells. *Scientific Reports* **7**, 45367
809 (2017). <https://doi.org:10.1038/srep45367>
810 56 Sato, T., Yamanishi, Y., Horimoto, K., Kanehisa, M. & Toh, H. Partial correlation
811 coefficient between distance matrices as a new indicator of protein-protein
812 interactions. *Bioinformatics* **22**, 2488-2492 (2006).
813 <https://doi.org:10.1093/bioinformatics/btl419>
814 57 Luck, K. *et al.* A reference map of the human binary protein interactome. *Nature*
815 **580**, 402-408 (2020). <https://doi.org:10.1038/s41586-020-2188-x>
816 58 Blohm, P. *et al.* Negatome 2.0: a database of non-interacting proteins derived by
817 literature mining, manual annotation and protein structure analysis. *Nucleic Acids*
818 *Research* **42**, D396-D400 (2014). <https://doi.org:10.1093/nar/gkt1079>
819 59 Fabregat, A. *et al.* The reactome pathway knowledgebase. *Nucleic acids*
820 *research* **46**, D649-D655 (2018).
821 60 Oughtred, R. *et al.* TheBioGRIDdatabase: A comprehensive biomedical resource
822 of curated protein, genetic, and chemical interactions. *Protein Science* **30**, 187-
823 200 (2021). <https://doi.org:10.1002/pro.3978>
824 61 Kanehisa, M., Sato, Y., Kawashima, M., Furumichi, M. & Tanabe, M. KEGG as a
825 reference resource for gene and protein annotation. *Nucleic Acids Research* **44**,
826 D457-D462 (2015). <https://doi.org:10.1093/nar/gkv1070>
827 62 Wright, E. S. Using DECIPHER v2. 0 to analyze big biological sequence data in
828 R. *R Journal* **8** (2016).
829 63 Vachaspati, P. & Warnow, T. ASTRID: Accurate Species TRees from Internode
830 Distances. *BMC Genomics* **16**, S3 (2015). [https://doi.org:10.1186/1471-2164-16-](https://doi.org:10.1186/1471-2164-16-s10-s3)
831 [s10-s3](https://doi.org:10.1186/1471-2164-16-s10-s3)
832 64 Biostrings: Efficient manipulation of biological strings. v. 2.68.0 (Bioconductor,
833 2023).
834 65 Team, R. C. R: A language and environment for statistical computing. (2013).
835 66 Brilli, M., Mengoni, A., Fondi, M., Bazzicalupo, M., Liò, P. & Fani, R. Analysis of
836 plasmid genes by phylogenetic profiling and visualization of homology
837 relationships using Blast2Network. *BMC Bioinformatics* **9**, 551 (2008).
838 <https://doi.org:10.1186/1471-2105-9-551>
839 67 Pellegrini, M., Marcotte, E. M., Thompson, M. J., Eisenberg, D. & Yeates, T. O.
840 Assigning protein functions by comparative genome analysis: Protein
841 phylogenetic profiles. *Proceedings of the National Academy of Sciences* **96**,
842 4285-4288 (1999). <https://doi.org:10.1073/pnas.96.8.4285>

843 68 Date, S. V. & Marcotte, E. M. Discovery of uncharacterized cellular systems by
844 genome-wide analysis of functional linkages. *Nature Biotechnology* **21**, 1055-
845 1062 (2003). <https://doi.org:10.1038/nbt861>

846 69 Beckley, A. M. & Wright, E. S. Identification of antibiotic pairs that evade
847 concurrent resistance via a retrospective analysis of antimicrobial susceptibility
848 test results. *The Lancet Microbe* **2**, e545-e554 (2021).

849 70 Fitch, W. M. On the problem of discovering the most parsimonious tree. *The*
850 *American Naturalist* **111**, 223-257 (1977).

851 71 Kryazhimskiy, S., Dushoff, J., Bazykin, G. A. & Plotkin, J. B. Prevalence of
852 Epistasis in the Evolution of Influenza A Surface Proteins. *PLoS Genetics* **7**,
853 e1001301 (2011). <https://doi.org:10.1371/journal.pgen.1001301>

854 72 Juan, D., Pazos, F. & Valencia, A. High-confidence prediction of global
855 interactomes based on genome-wide coevolutionary networks. *Proceedings of*
856 *the National Academy of Sciences* **105**, 934-939 (2008).
857 <https://doi.org:10.1073/pnas.0709671105>

858 73 Sato, T., Yamanishi, Y., Kanehisa, M. & Toh, H. The inference of protein-protein
859 interactions by co-evolutionary analysis is improved by excluding the information
860 about the phylogenetic relationships. *Bioinformatics* **21**, 3482-3489 (2005).
861 <https://doi.org:10.1093/bioinformatics/bti564>

862 74 Altschul, S. F., Gish, W., Miller, W., Myers, E. W. & Lipman, D. J. Basic local
863 alignment search tool. *J Mol Biol* **215**, 403-410 (1990).
864 [https://doi.org:10.1016/s0022-2836\(05\)80360-2](https://doi.org:10.1016/s0022-2836(05)80360-2)

865 75 Achlioptas, D. in *Proceedings of the twentieth ACM SIGMOD-SIGACT-SIGART*
866 *symposium on Principles of database systems*. 274-281.

867 76 Steel, M. A. & Penny, D. Distributions of Tree Comparison Metrics—Some New
868 Results. *Systematic Biology* **42**, 126-141 (1993).
869 <https://doi.org:10.1093/sysbio/42.2.126>

870 77 Korbel, J. O., Jensen, L. J., Von Mering, C. & Bork, P. Analysis of genomic
871 context: prediction of functional associations from conserved bidirectionally
872 transcribed gene pairs. *Nature biotechnology* **22**, 911-917 (2004).

873 78 Philip, J. The probability distribution of the distance between two random points
874 in a box. *KTH Mathematics, Royal Institute of Technology* (2007).

875 79 Gittleman, J. L. & Kot, M. Adaptation: Statistics and a Null Model for Estimating
876 Phylogenetic Effects. *Systematic Biology* **39**, 227-241 (1990).
877 <https://doi.org:10.2307/2992183>

878 80 Cliff, A. & Ord, J. *Spatial Processes* (London: Pion). *Google Scholar* (1981).

879 81 Pesaranghader, A., Matwin, S., Sokolova, M., Grenier, J.-C., Beiko, R. G. &
880 Hussin, J. deepSimDEF: deep neural embeddings of gene products and Gene
881 Ontology terms for functional analysis of genes. *Bioinformatics* (2022).
882 <https://doi.org:10.1093/bioinformatics/btac304>

883 82 Soleymani, F., Paquet, E., Viktor, H. L., Michalowski, W. & Spinello, D.
884 ProtInteract: a Deep Learning Framework for Predicting Protein—Protein
885 Interactions. *Computational and Structural Biotechnology Journal* (2023).
886 <https://doi.org:https://doi.org/10.1016/j.csbj.2023.01.028>

887 83 Ekeberg, M., Hartonen, T. & Aurell, E. Fast pseudolikelihood maximization for
888 direct-coupling analysis of protein structure from many homologous amino-acid
889 sequences. *Journal of Computational Physics* **276**, 341-356 (2014).
890 <https://doi.org/10.1016/j.jcp.2014.07.024>

891 84 Jones, D. T., Buchan, D. W. A., Cozzetto, D. & Pontil, M. PSICOV: precise
892 structural contact prediction using sparse inverse covariance estimation on large
893 multiple sequence alignments. *Bioinformatics* **28**, 184-190 (2011).
894 <https://doi.org/10.1093/bioinformatics/btr638>

895 85 Buslje, C. M., Santos, J., Delfino, J. M. & Nielsen, M. Correction for phylogeny,
896 small number of observations and data redundancy improves the identification of
897 coevolving amino acid pairs using mutual information. *Bioinformatics* **25**, 1125-
898 1131 (2009).

899 86 Liaw, A. & Wiener, M. Classification and Regression by randomForest. *R News*
900 **2**, 18-22 (2002).

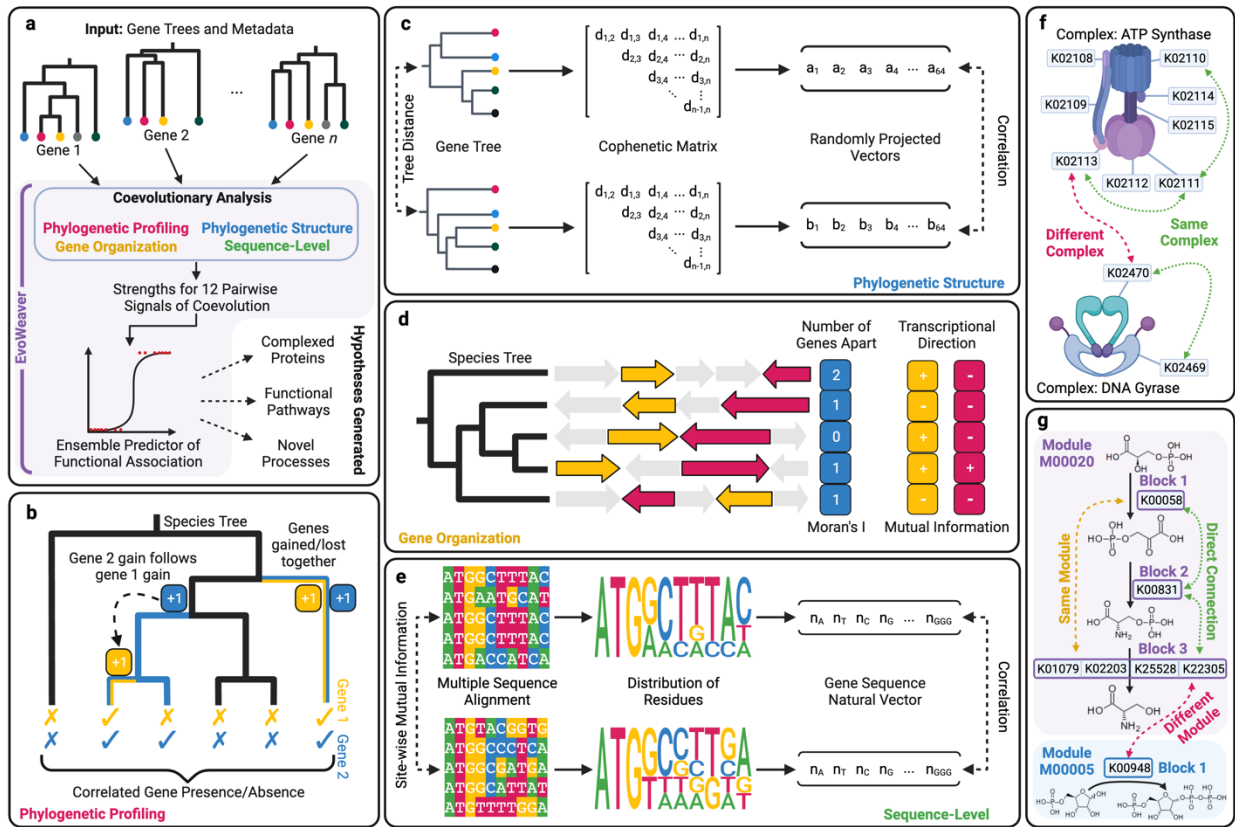
901 87 Strobl, C., Boulesteix, A.-L., Zeileis, A. & Hothorn, T. Bias in random forest
902 variable importance measures: Illustrations, sources and a solution. *BMC*
903 *Bioinformatics* **8**, 25 (2007). <https://doi.org/10.1186/1471-2105-8-25>

904 88 Csárdi, G. & Nepusz, T.

905 89 Gentleman, R. C. *et al.* Bioconductor: open software development for
906 computational biology and bioinformatics. *Genome biology* **5**, 1-16 (2004).

907 90 OSG. (ed OSG) (2015).

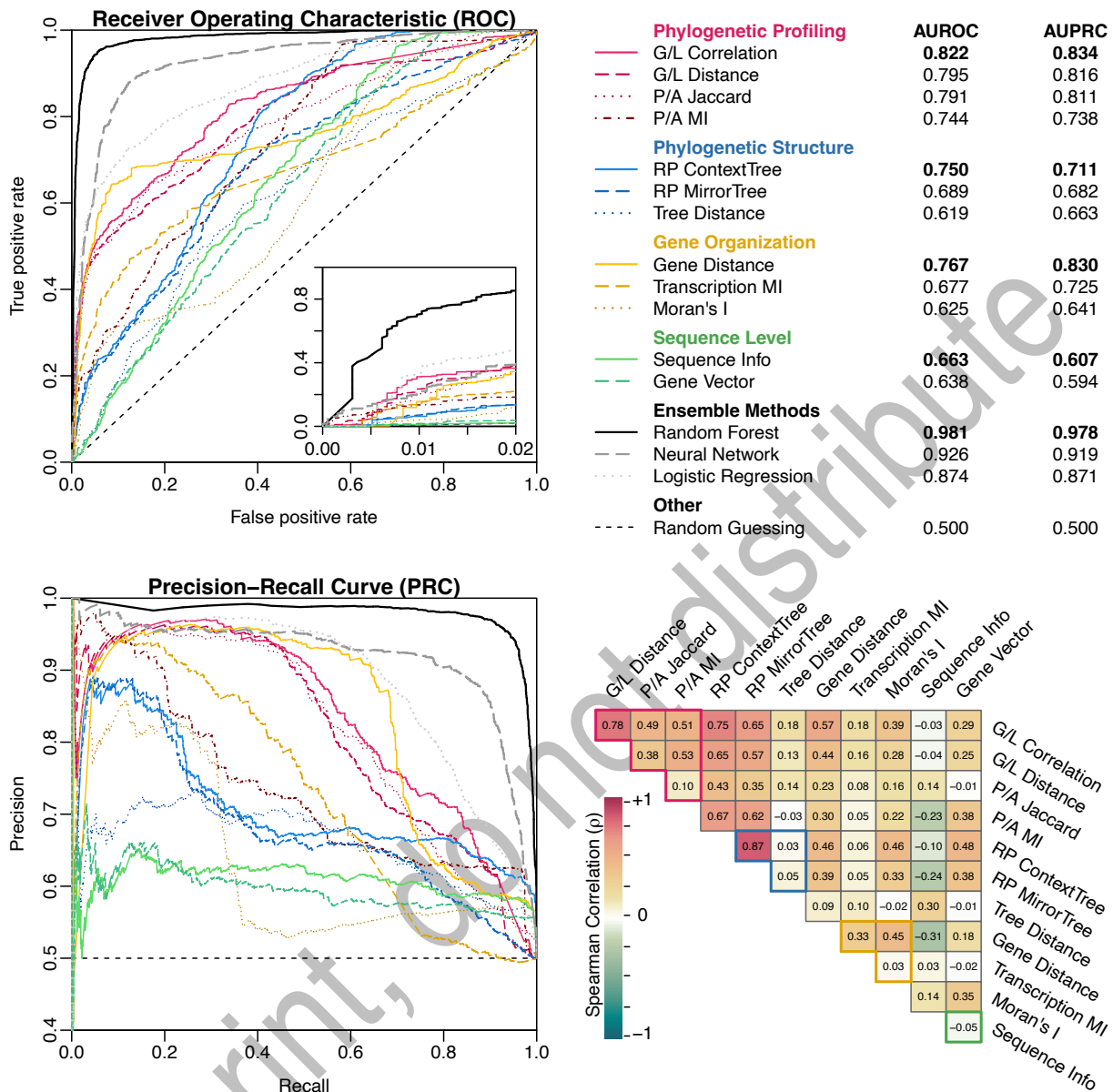
908



911
912 **Figure 1: Overview of the EvoWeaver algorithm and benchmarking. (a)**
913 Phylogenetic trees from gene orthologs serve as the primary input to EvoWeaver. Four
914 categories of coevolutionary signal are quantified for each pair of genes. These signals
915 are combined in an ensemble classifier to predict functional relationships between gene
916 pairs. **(b)** Functional associations often result in correlated gain/loss patterns on a
917 phylogenetic tree of the species. EvoWeaver assesses the presence/absence patterns,
918 correlation between gain/loss events, and distance between gain/loss events as signals
919 of coevolution. **(c)** Similarity in phylogenetic structure is another indicator of coevolution
920 between genes. EvoWeaver computes topological distance as well as correlation in
921 patristic distances following dimensionality reduction using random projection. **(d)**
922 Functionally associated genes sometimes cluster on the genome due to co-regulation or
923 horizontal gene transfer. EvoWeaver derives signals from the conservation in
924 transcriptional direction and the distance between gene pairs. **(e)** Functional
925 associations sometimes cause concerted changes in sequences that are interrogated
926 by EvoWeaver. **(f)** Proteins involved in the same complex are functionally associated
927 and can be identified through signals of coevolution. The goal of the Complexes
928 benchmark is to distinguish orthology groups in the same complex (i.e., positives) from
929 those in different complexes (i.e., negatives). **(g)** Functional associations between
930 proteins that are adjacent in the same module are stronger than those between different

931 modules. The goal of the Modules benchmark is to distinguish adjacent proteins in the
932 same module from independent modules.

Preprint, do not distribute

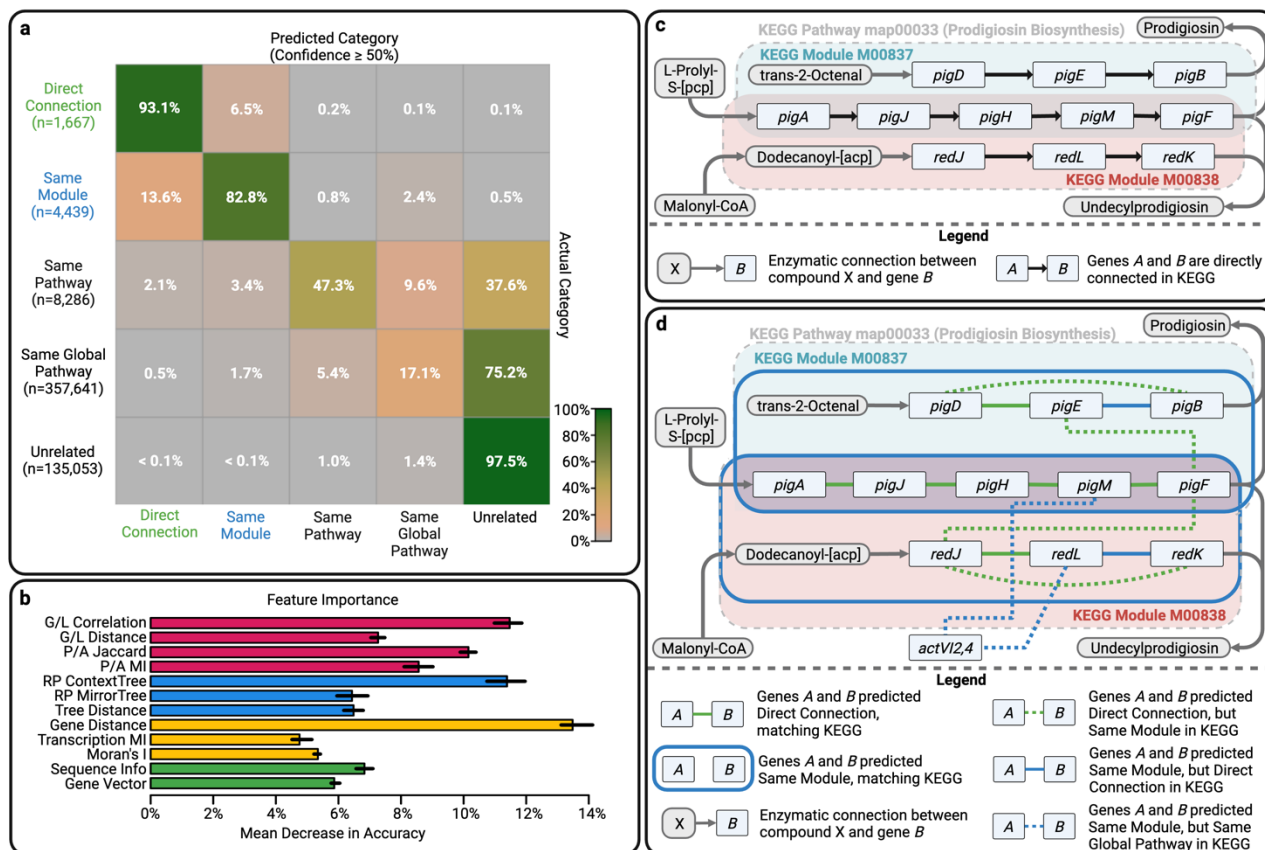


933

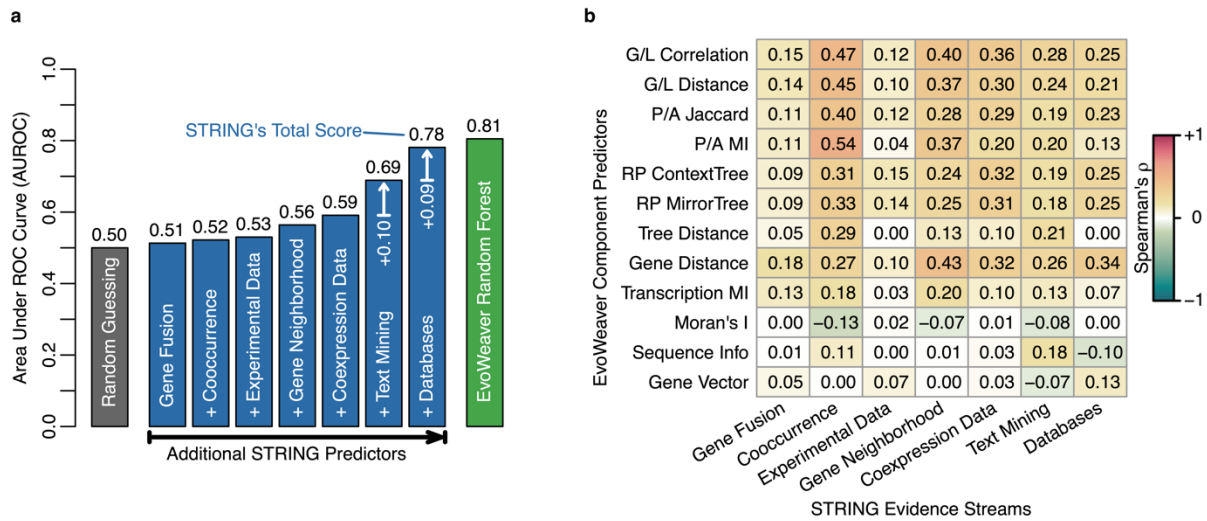
934 **Figure 2: EvoWeaver's ensemble predictions outperform individual algorithms on**
 935 **the Modules benchmark.** Coevolutionary approaches were compared for their ability to
 936 discern adjacent proteins in KEGG modules (i.e., 1,948 positives) from proteins in
 937 distinct modules (i.e., 1,948 negatives). No single source of coevolutionary signal
 938 greatly outcompeted all other sources. However, EvoWeaver's ensemble predictions
 939 that combine all component sources of coevolutionary signal substantially improved
 940 predictive accuracy, as seen by larger areas under the curves. Inset of the receiver
 941 operating characteristic highlights the region with low false positive rates. Scores from
 942 individual algorithms tended to have low correlation except within similar categories of
 943 coevolutionary signal (i.e., boxed groups in the heatmap), suggesting that the ensemble
 944 approach is superior because it combines quasi-orthogonal coevolutionary signals.

945 Spearman's correlation from positive and negative sets is averaged to correct for
946 artificial correlation among high performing algorithms.

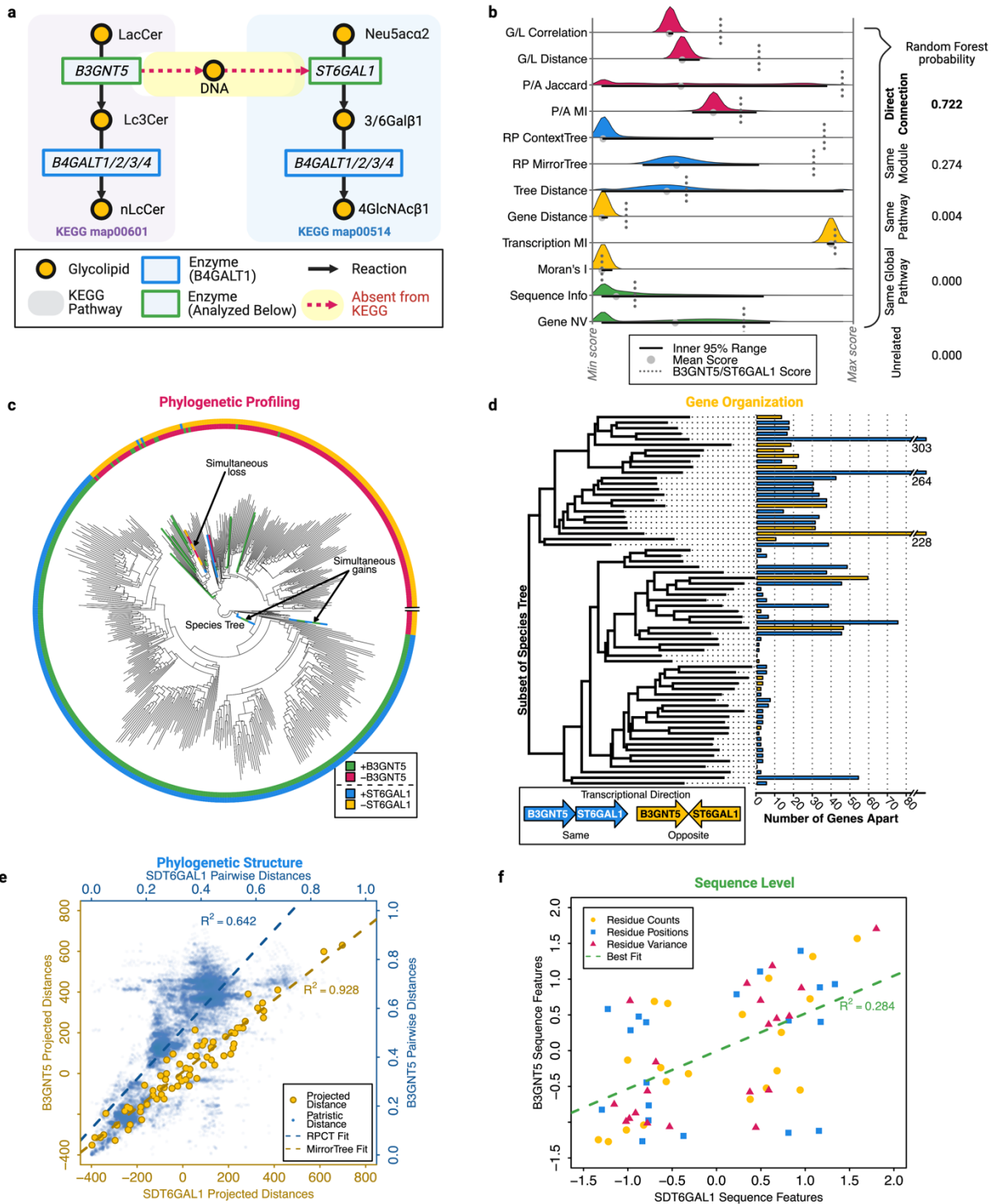
Preprint, do not distribute



947 **Figure 3: EvoWeaver is sufficiently accurate to hierarchically classify functional**
 948 **associations. (a)** The confusion matrix of five level classifications indicates that
 949 EvoWeaver's ensemble predictions (i.e., random forest) rarely confuse proteins within
 950 the same module with those from different modules. Values represent the percent of
 951 each actual category classified to each predicted category. **(b)** The best performing
 952 algorithm from each category on the Modules benchmark also was assigned greater
 953 feature importance by the random forest model in hierarchical classification. All features
 954 were important in the ensemble's predictions, further underscoring the benefit of using
 955 multiple coevolutionary signals. Error bars denote the range of importances across each
 956 train/test fold. **(c-d)** Hierarchical classifications permit the partial inference of
 957 biochemical pathways directly from sequence information without any external biological
 958 knowledge. EvoWeaver's ensemble predictions for genes involved in prodigiosin
 959 biosynthesis generally match experimentally verified connections in KEGG. Panel (c)
 960 displays the original pathway from KEGG, and panel (d) overlays EvoWeaver's
 961 hierarchical classifications. Note that *pigA*, *pigJ*, *pigH*, *pigM*, and *pigF* belong to both
 962 modules.
 963



964
 965 **Figure 4: EvoWeaver outperforms STRING without reliance on external data. (a)**
 966 Predictive accuracy was compared on 6,892 pairs of gene groups that overlapped
 967 between STRING and the Modules benchmark. Area under the ROC curve (AUROC) is
 968 shown for discerning between pairs sharing the same non-global pathway in KEGG
 969 (i.e., positives) versus pairs in different non-global pathways (i.e., negatives). STRING's
 970 predictions are a composite of seven evidence streams, including three coevolutionary
 971 evidence streams (i.e., Gene Fusion, Cooccurrence, Gene Neighborhood). Sequentially
 972 incorporating evidence streams from least to most beneficial demonstrates their
 973 marginal impact on STRING's reported Total Score. Text Mining and Databases were
 974 the most impactful evidence streams. Despite STRING's predictions incorporating
 975 KEGG into its Databases evidence stream, EvoWeaver's Random Forest predictions
 976 outperformed STRING's Total Score while only using sequence information. **(b)**
 977 Unsurprisingly, some of EvoWeaver's component predictors were modestly correlated
 978 with STRING's evidence streams. For example, STRING's Cooccurrence score, based
 979 on SVD-phy, is correlated with EvoWeaver's phylogenetic profiling methods, and
 980 STRING's Gene Neighborhood score is correlated with EvoWeaver's Gene Distance
 981 predictor. Spearman's correlation is calculated in the same manner as in Figure 2.



982

983 **Figure 5: EvoWeaver's ensemble predictions can generate high fidelity biological**

984 **hypotheses. (a)** The protein product of *B3GNT5* promotes the expression of

985 *ST6GAL1*⁵⁵, although this connection is missing in KEGG and STRING. **(b)**

986 EvoWeaver's component and ensemble predictions indicate that *B3GNT5* and

987 *ST6GAL1* are functionally associated, which is supported by experiments in human cell
988 culture⁵⁵. **(c)** Phylogenetic profiling demonstrates a pattern of association between
989 *B3GNT5* and *ST6GAL1*, although it is supported by relatively few gain/loss events on
990 the species tree. **(d)** Organisms with both *B3GNT5* and *ST6GAL1* on the same
991 chromosome display a clear linkage in gene distance and transcriptional direction. **(e)**
992 Shared patristic distances from both gene trees are correlated, especially after
993 compression with random projection, suggesting a high degree of coevolution between
994 *B3GNT5* and *ST6GAL1*. **(f)** Gene sequence natural vectors for both *B3GNT5* and
995 *ST6GAL1* are moderately correlated, implying similar residue compositions and
996 providing further signal of coevolution.

Preprint, do not distribute

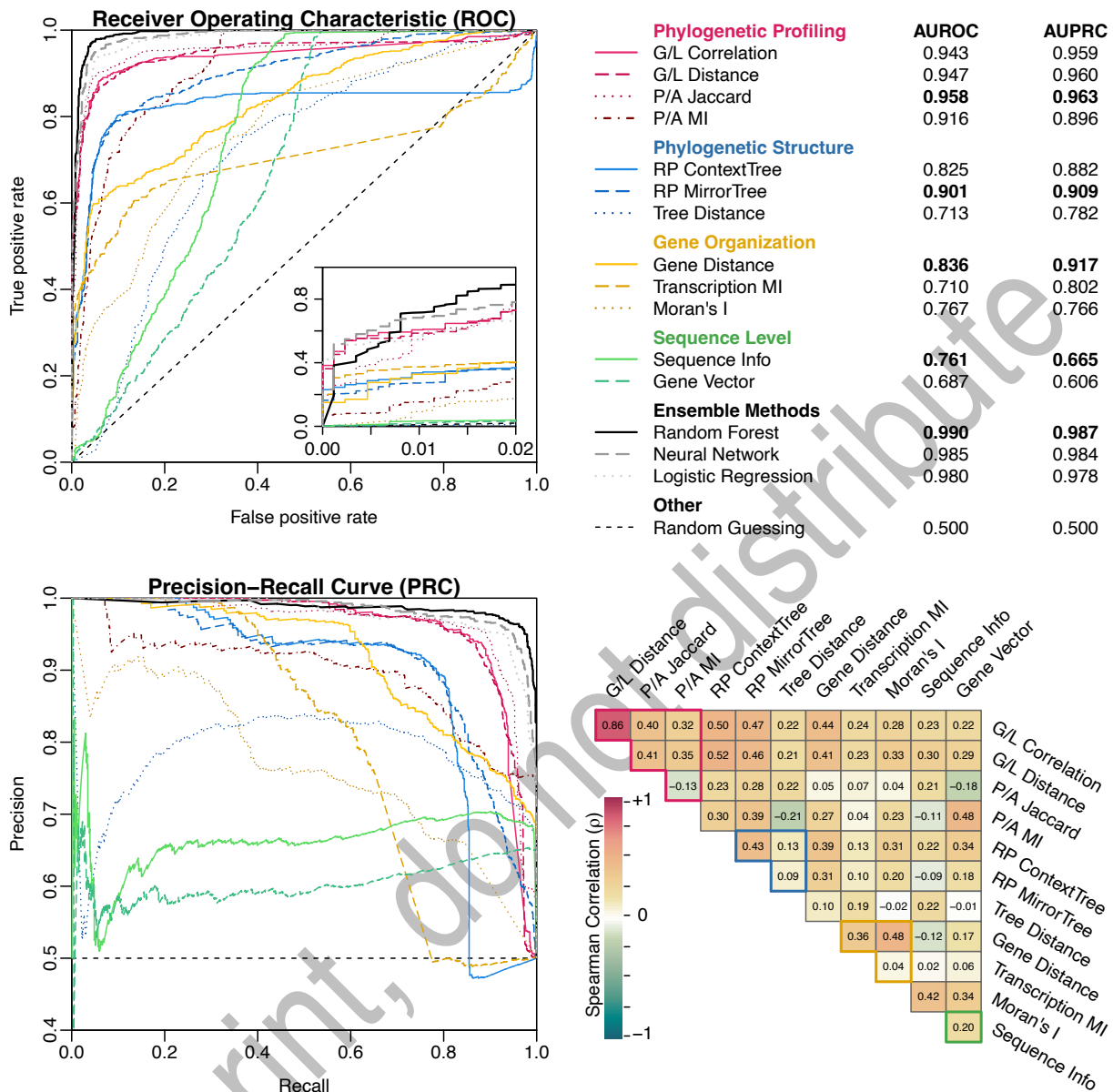
Symbol	Meaning	Example	Interpretation	Example Module
K12345	Orthology group #12345	K05308	Each code is comprised of "K" followed by a unique 5-digit string. K05308 encodes gene <i>gnaD</i>	Any
Space	Direct connection	K05308 K18126	K05308 performs/facilitates a chemical reaction immediately prior to K18126	M00633
Plus (+)	Complex	K02111+K02112	K02111 and K02112 belong to the same complex	M00157
Minus (-)	Optional Complex	-K03944	K03944 is an optional component of the complex	M00143
Parentheses	Optional Components	(K01681,K01682)	Either K01681 or K01682 performs/facilitates this chemical reaction	M00012
Newline	Separate Components	K21428 K21778 K21779 K21787	K21779 and K21787 are in the same module, but they participate in different stages of the module	M00837

997

998

999

Table S1: Description of KEGG Modules. Each module in KEGG is specified with a plain text definition composed of orthology groups and symbols specifying relationships.



1000

1001

1002

1003

1004

1005

1006

1007

1008

1009

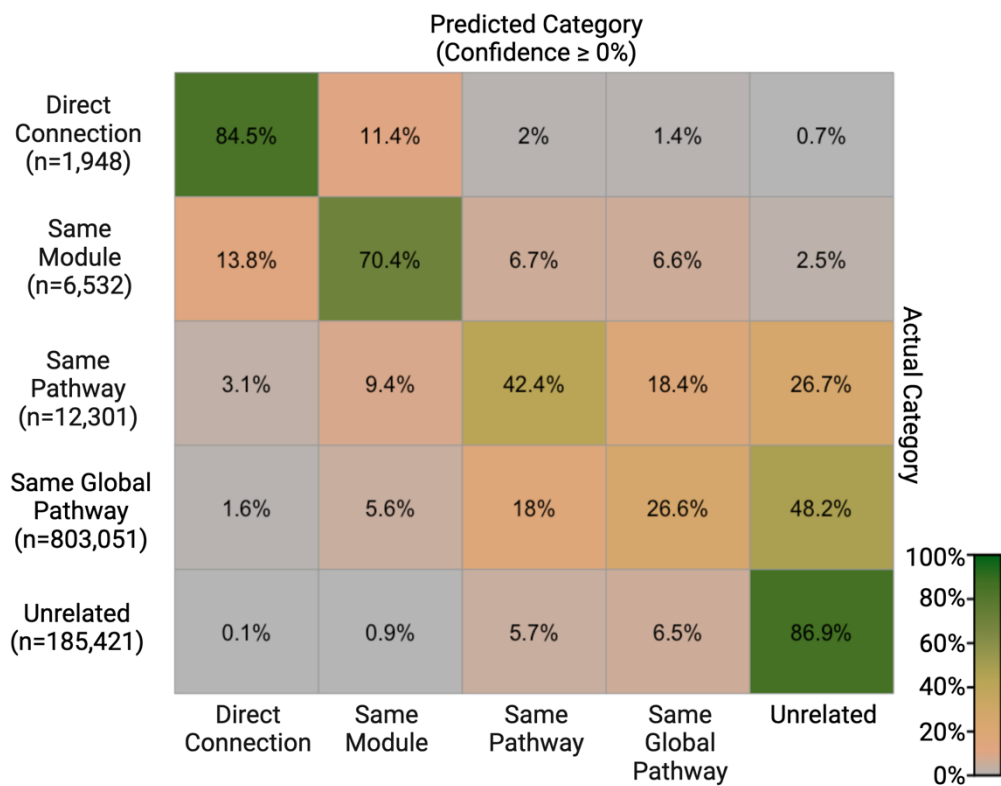
1010

1011

Figure S1: EvoWeaver's ensemble predictions outperform individual algorithms on the Complexes benchmark. Coevolutionary approaches were compared for their ability to discern pairs of KO groups that complex (i.e., 867 positives) from unrelated pairs of KO groups (i.e., 867 negatives). Phylogenetic profiling algorithms tended to outperform other methods, though all categories of analysis showed strong performance. EvoWeaver's ensemble predictions that combine all component sources of coevolutionary signal improved predictive accuracy, as seen by larger areas under the curves. Inset of the receiver operating characteristic highlights the region with low false positive rates. Scores from individual algorithms tended to have low correlation except within similar categories of coevolutionary signal (i.e., boxed groups in the heatmap), suggesting that the ensemble approach is superior because it combines

1012 quasi-orthogonal coevolutionary signals. Spearman's correlation from positive and
1013 negative sets is averaged to correct for artificial correlation among high performing
1014 algorithms.

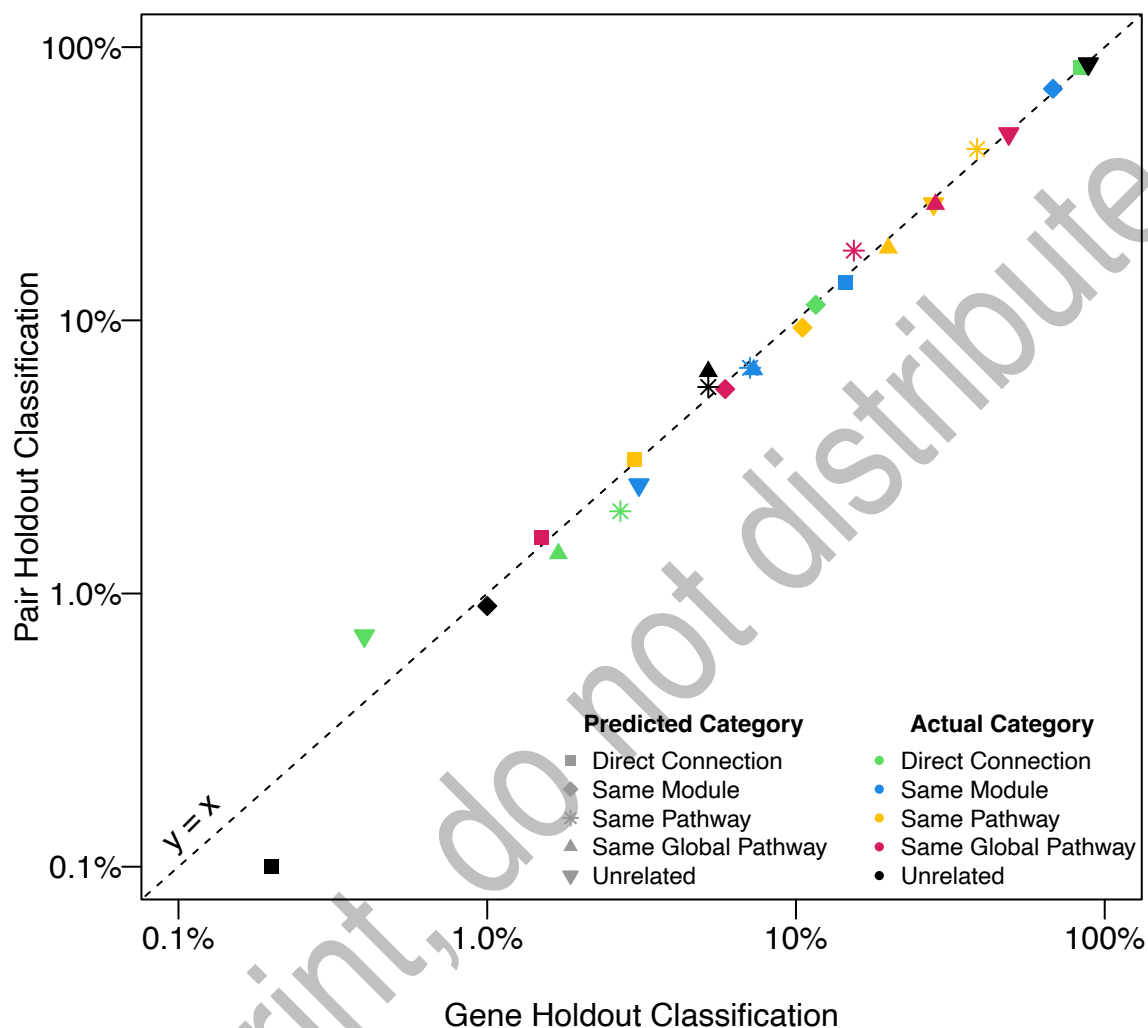
Preprint, do not distribute



1015
1016
1017
1018
1019
1020
1021

Figure S2: EvoWeaver’s hierarchical classifications at any confidence level. Each gene group pairing was assigned to its highest confidence predicted category without imposing a minimum confidence threshold. Results are analogous to Fig. 3a, except with more pairs predicted in the Same Global Pathway category and slightly higher misclassification rates.

Gene Holdout vs. Pair Holdout Multiclass Results



1022
1023 **Figure S3: EvoWeaver’s hierarchical classifications are consistent using gene**
1024 **holdouts or gene pair holdouts.** Each point denotes the percentage of pairs in each
1025 actual category (point color) classified to each predicted category (point shape). The
1026 dashed identity line (i.e., $y=x$) represents a scenario of perfect consistency between the
1027 two evaluations. Note the log scaled axes used for visual clarity. Resulting
1028 classifications are almost identical between holdout approaches, implying that
1029 EvoWeaver is not simply learning to identify highly connected gene groups.